JOURNAL OF SOLID STATE CHEMISTRY 78, 232–236 (1989)

# Site Selective Laser Spectroscopy Study of Defect Equilibria in MgO : $Cr^{3+}$

JEFFREY R. POLIAK, KATHLEEN R. NOON, AND JOHN C. WRIGHT*

*Department of Chemistry, University of Wisconsin, Madison, Wisconsin 53706*

Received August 12, 1988; in revised form September 30, 1988

Aliovalent $Cr^{3+}$ dopants in MgO are compensated either locally or distantly by magnesium vacancies. The relative concentrations of the two $Cr^{3+}$ sites are measured as a function of dopant concentration by site selective laser spectroscopy. The locally compensated site concentration increases dramatically as the dopant concentration is raised. The increase can be described by a mass action relationship for the pairing equilibrium between the dopant and its charge compensation. This behavior is in marked contrast to the defect equilibria in fluorite compounds where the site concentrations do not follow simple mass action relationships. © 1989 Academic Press, Inc.

## Introduction

The optical and epr spectroscopy of MgO : $Cr^{3+}$ has been studied previously by a number of workers (*1–19*). The extra charge of the $Cr^{3+}$ ($Cr_{Mg}^{\cdot}$ using the Kroger–Vink notation (*20*) is compensated by a magnesium vacancy ($V_{Mg}''$) which can occupy different crystallographic sites relative to $Cr_{Mg}^{\cdot}$. The five major sites are summarized in Fig. 1 along with the label that identifies the sites in this paper and the wavelength of the dominant fluorescence lines for that site. The A site is a $Cr_{Mg}^{\cdot}$ distantly compensated by a $V_{Mg}''$ while the B site is a locally compensated $(Cr_{Mg} \cdot V_{Mg})'$ with tetragonal symmetry. Both sites have the $Cr^{3+}$ $^2E_g$ state as the first excited state. This state interacts weakly with the crystal fields and the fluorescence transitions are sharp. There is also a rhombic symmetry $(Cr_{Mg} \cdot V_{Mg})'$ site that has only broad fluorescence transitions because the strongly interacting $^4T_{2g}$ state is the first excited state.

When a $V_{Mg}''$ is associated with two $Cr_{Mg}^{\cdot}$, a $(2Cr_{Mg} \cdot V_{Mg})^x$ dimer is formed. It is a neutral, linear defect with the $V_{Mg}''$ in a next-nearest-neighbor position to both $Cr_{Mg}^{\cdot}$ so all three lie along a (100) axis (*6, 17–19, 21, 22*). It is labeled site C in this paper. A number of different studies have shown that the properties of this center and the tetragonal $(Cr_{Mg} \cdot V_{Mg})'$ center are similar. The two lines at 698.9 and 703.6 nm are assigned to the splitting of the $^2E_g$ state.

The last site in Fig. 1 has been suggested to be a $V^-$ center consisting of a hole trapped on an oxygen neighboring a $V_{Mg}''$ (*9*). Two lines are seen in excitation spectra at ca. 699.7 and 700.0 nm (*9, 23*) and these lines will be labeled D1 and D2 in this pa-

* To whom correspondence should be addressed.

0022-4596/89 $3.00

per. It is not known whether they come from a single ion or two ions in different sites.

In this paper, we present the results of measuring the relative concentrations of the different sites for different annealing conditions and different dopant concentrations. We have found that the D1 and D2 lines are strongly dependent on annealing conditions but the other sites do not have any observable dependence. The dimer sites do not become important until concentrations above 0.1 mole%. The relative importance of the A and B sites is strongly dependent on doping concentration. As the dopant concentration is raised from low values, one expects an increase in the concentration of $V''_{Mg}$ since pairing with the $Cr^{\cdot}_{Mg}$ is not large. An increase in $V''_{Mg}$ causes increased association between $V''_{Mg}$ and $Cr^{\cdot}_{Mg}$ so the ratio of $[(Cr_{Mg} \cdot V_{Mg})']/[(Cr^{\cdot}_{Mg}]$ should increase proportionately. This behavior is observed experimentally. It can be described by using a mass action relationship for the pairing equilibrium. The system is quite similar to that observed for CaO : $Eu^{3+}$ (*24*).

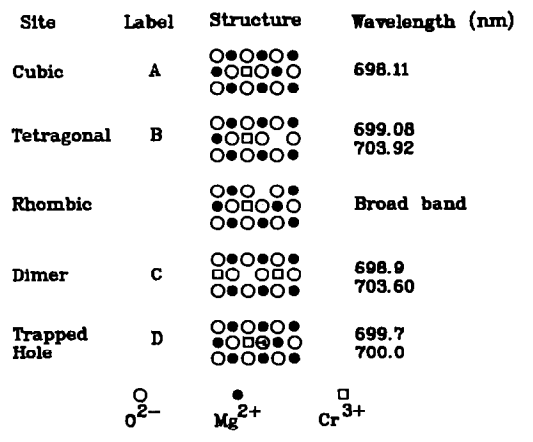


FIG. 1. Diagram of the defect sites for MgO : $Cr^{3+}$.

## Experimental

MgO samples were prepared by precipitation of 1.2 *M* $Mg(NO_3)_2$ (Spex, 99.999%) with 0.3 *M* electronic-grade $NH_4OH$ (Hi-Pure Chemicals, Inc.). Different amounts of $3 \times 10^{-3}$ *M* $Cr(NO_3)_3 \cdot 9H_2O$ (Spex, 99.99%) were added depending on the desired mole% of Cr in MgO. The $Cr^{3+}$ concentrations in the final samples were assumed to be the same as the $Cr^{3+}/Mg^{2+}$ ratio in solution. After aging, the precipitates were filtered, washed, dried at room temperature, ground, and ignited for at least 10 hr at 1100–1200°C in a tube furnace.

$Cr^{3+}$ fluorescence was excited with a nitrogen laser pumped dye laser which had a bandwidth of 0.02 nm. Samples were pelletized in a copper sample holder that was cooled to 12 K with a closed cycle cryogenic refrigerator. Fluorescence was measured with either a 1- or ¼-m monochromator depending upon whether high-resolution fluorescence spectra of single sites or the excitation spectra of all sites were required. Fluorescence spectra from all sites were measured by exciting at 550 nm where the A, B, and C site transitions are broad and overlapping. Temporal discrimination was used to separate the laser beam from the resonant fluorescence. Since the fluorescence lifetimes are long, a mechanical chopper was used to trigger the laser. When it was positioned in front of the monochromator slits, it obstructed light from the laser but passed the long-lived fluorescence as the wheel rotated away from the slits.

## Results

Example spectra for a 0.1 mole% $Cr^{3+}$ sample are shown in Fig. 2. Figure 2a shows the excitation spectrum obtained by scanning the dye laser over the $^4A_{2g} \rightarrow {}^2E_g$ transition while monitoring the fluorescence with the ¼-m monochromator. Figure 2b shows the $^2E_g \rightarrow {}^4A_{2g}$ fluorescence spec-

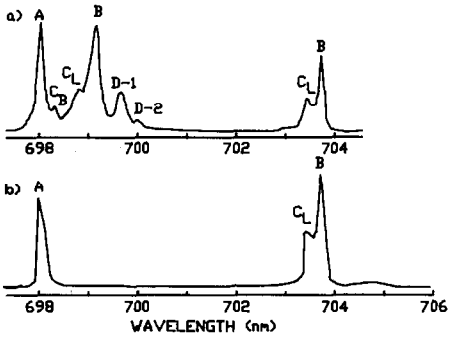


FIG. 2. (a) The $^4A_{2g} \rightarrow {}^2E_g$ excitation spectrum of $MgO:Cr^{3+}$ showing the positions of the important lines while monitoring sample fluorescence at 700 m with a low resolution monochromator. (b) The $^2E_g \rightarrow {}^4A_{2g}$ fluorescence spectrum of $MgO:Cr^{3+}$ while exciting the sample at 550 nm.

trum while exciting the $^4T_{2g}$ broad absorption band at 550 nm. The transitions for the individual sites sketched in Fig. 1 are indicated with letters on Fig. 2. The spectra are dependent on the annealing conditions and the dopant concentrations. In particular, the D1 and D2 lines that have been attributed to a hole compensated site can vary greatly for different preparation conditions. Figure 3 shows the fluorescence and excitation spectra for samples that were prepared under a mixed $Ar/H_2$ atmosphere in a quartz tube. The relative intensity of the D1 and D2 transitions is not reproducible for seemingly identical sample preparations but the other sites are reproducible. We therefore sought conditions that would minimize the importance of the D1 and D2 lines so the defect equilibria of interest would not be affected. We found that igniting the samples in a $N_2$ atmosphere and an alumina tube resulted in spectra that had small but constant contributions from these lines. The spectra indicated that the contributions were sufficiently small that the defect equilibria involving the $V''_{Mg}$ compensation would not be affected. The remaining work was done under these conditions.

The excitation spectra were measured with broadband fluorescence monitoring for a number of different concentrations of $Cr^{3+}$. Example spectra are shown in Fig. 4. At low concentrations of total $Cr^{3+}$, only the cubic (A) site is present. The concentration of this site increases roughly linearly as the $Cr^{3+}$ concentration increases. In general, the formation of the $(Cr_{Mg} \cdot V_{Mg})'$ (B) site is apparent above concentrations of

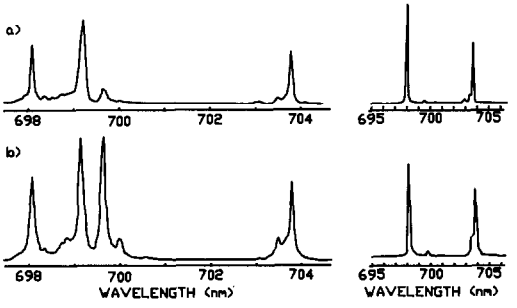


FIG. 3. Excitation (left side) and fluorescence spectra (right side) of $MgO:Cr^{3+}$ samples that had been annealed in a mixed $Ar/H_2$ atmosphere. The spectra in (a) and (b) were two separate samples treated identically. The excitation spectra were taken while monitoring sample fluorescence at 700 nm with a low-resolution monochromator. Fluorescence spectra were taken while exciting the sample at 550 nm.

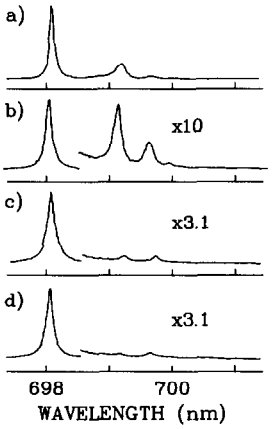


FIG. 4. Excitation spectra for $MgO:Cr^{3+}$ samples with $Cr^{3+}$ concentrations of (a) 0.098, (b) 0.074, (c) 0.049, (d) 0.0098 mole%. Sample fluorescence was measured at 700 nm with a low-resolution monochromator.

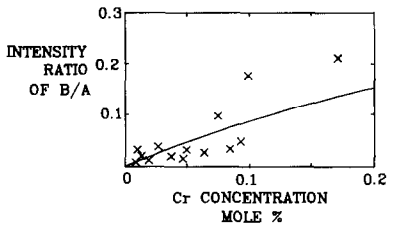


FIG. 5. Ratio of the site B/A intensities as a function of dopant concentration (mole%). The points are experimental data while the line represents the theoretical model explained in the text.

0.01 mole%. Between 0.02 and 0.1 mole%, the $(2Cr_{Mg} \cdot V_{Mg})^x$ dimer begins to be important. There is no consistent concentration dependence observed for the D1 and D2 transitions. The B/A concentration ratio was followed over the range of concentrations by measuring the ratio of the peak intensities of the 699.1-nm tetragonal site line and the 698-nm cubic site line. The results are shown in Fig. 5. It was not possible to obtain consistent values for the ratio. The results in Fig. 5 are the average of a number of measurements. The scatter is attributed to the inability to control the defect concentrations at low dopant levels where there is great sensitivity to aliovalent impurities present from the original precipitation conditions or introduced in the furnace during the annealing. Despite the scatter, there is clearly a dramatic increase in the concentration of the $(Cr_{Mg} \cdot V_{Mg})'$ site as the dopant concentration is raised.

## Discussion

The defect chemistry can be described by a mass action relationship for the pairing equilibrium, the charge balance condition, and mass balance. We neglect the intrinsic defect equilibrium and any contributions from aliovalent impurities.

$$K = \frac{[(Cr_{Mg} \cdot V_{Mg})']}{[Cr_{Mg}^{\cdot}][V''_{Mg}]} \quad (1)$$

$$2[V''_{Mg}] + [(Cr_{Mg} \cdot V_{Mg})'] = [Cr_{Mg}^{\cdot}] \quad (2)$$

$$C_{Cr} = [Cr_{Mg}^{\cdot}] + [(Cr_{Mg} \cdot V_{Mg})'] \quad (3)$$

These equations are solved for the defect concentrations and the ratio of $[Cr_{Mg} \cdot V_{Mg})']/[Cr_{Mg}^{\cdot}]$ is calculated for total $Cr^{3+}$ concentrations over the range shown in Fig. 5. The results are shown as the solid line. They assume a value for $K$ of 210 (mole fraction)$^{-1}$ and a ratio of the relative site intensities $(I_B/I_A)$ to the relative concentration ratio of 1.0. The choices for these parameters are not well-constrained since smaller values of $K$ can give suitable fits if larger values are chosen for the intensity/concentration proportionality. Nevertheless, the defect model predictions are consistent with the experimentally observed variation in the associated pair/cubic site intensities. The model predicts that an increased $Cr^{3+}$ concentration raises the $V''_{Mg}$ concentration which causes an increase in the $[(Cr_{Mg} \cdot V_{Mg})']/[Cr_{Mg}^{\cdot}]$ ratio from Eq. 1. At high $Cr^{3+}$ concentrations $(C_{Cr} \gg 1/K)$, the ratio should approach unity where $Cr_{Mg}^{\cdot}$ compensate the $(Cr_{Mg} \cdot V_{Mg})'$ sites. At very low concentrations, the cubic site is the only appreciable defect observed. In this region, the concentration of the associated pair site is determined by impurities that provide a background concentration of $V''_{Mg}$. In the range for these experiments, $[Cr_{Mg}^{\cdot}] \gg [(Cr_{Mg} \cdot V_{Mg})']$ and the ratio $[(Cr_{Mg} \cdot V_{Mg})']/[Cr_{Mg}^{\cdot}]$ is approximately $KC_{Cr}/2$.

## Conclusions

The site distribution changes are quite similar to those observed in $CaO : Eu^{3+}$[24]. $CaO : Eu^{3+}$ has the same type of cubic and associated pair sites and the concentration dependence is described by the same model with a $K$ of 3000 (mole fraction)$^{-1}$. Both systems are quite different from the variations seen in the fluorites (*25–28*). In the fluorites, the cubic/associated pair site in-

tensities actually increased as the total dopant concentration was raised. The anomalous behavior in the fluorites was ascribed to nonideality corrections that were augmented by strain fields that caused additional interactions between defects (*28*). It was suggested that these strain fields were also responsible for the fluorites' superionic conductivity where the nonidealities caused a thermodynamic instability (*29–31*). Neither MgO nor CaO exhibit superionic conductivity at the temperatures used for these experiments and it is clear that the nonidealities do not play as important a role. The defect distributions are consistent with traditional mass action relationships.

## Acknowledgment

This research was supported by the Solid State Chemistry Program of the National Science Foundation under Grant DMR-8645405.

## References

1. O. Deutschbein, *Annal. Phys.* **20,** 282 (1934).
2. W. Low, *Phys. Rev.* **105,** 801 (1957).
3. J. E. Wertz and P. Auzins, *Phys. Rev.* **106,** 484 (1957).
4. J. H. E. Griffiths and J. W. Orton, *Proc. R. Soc. London* **73,** 1948 (1959).
5. S. Sugano, A. L. Schawlow, and F. Varsanyi, *Phys. Rev.* **120,** 2045 (1960).
6. G. F. Imbusch, A. L. Schawlow, A. D. May, and S. Sugano, *Phys. Rev.* **140,** A830 (1965).
7. A. L. Schawlow, A. H. Piksis, and S. Sugano, *Phys. Rev.* **122,** 1469 (1961).
8. A. L. Schawlow, *J. Appl. Phys. Suppl.* **33,** 395 (1962).
9. A. M. Glass, *J. Chem. Phys.* **46,** 2080 (1967).
10. J. P. Larkin, G. F. Imbusch, and F. Dravnieks, *Phys. Rev. B* **7,** 495 (1973).
11. K. P. O'Donnell, M. O. Henry, B. Henderson, and D. O'Connell, *J. Phys. C* **10,** 3877 (1977).
12. F. Castelli and L. S. Foster, *Phys. Rev. B* **11,** 920 (1975).
13. M. O. Henry, J. P. Larkin, and G. F. Imbusch, *Phys. Rev. B* **13,** 1893 (1976).
14. C. Mc Donagh, P. Dawson, and B. Henderson, *J. Phys. C* **13,** 2191 (1980).
15. K. Rabia, A. Boyrivent, and E. Duval, *J. Phys. C* **18,** 1975 (1985).
16. B. D. Mac Craith, T. J. Glynn, G. F. Imbusch, and C. Mc Donagh, *J. Phys. C* **13,** 4211 (1980).
17. A. Boyrivent, M. Ferrari, E. Duval, and A. Monteil, *J. Phys. C* **19,** 3253 (1986).
18. M. B. O'Neill and B. Henderson, *J. Lumin.* **39,** 161 (1988).
19. M. B. O'Neill and B. Henderson, *J. Lumin.* **39,** 239 (1988).
20. F. A. Kroger and H. J. Vink, "Solid State Physics" (F. Seitz and D. Turnbull, Eds.), Vol. 3, Academic Press, New York (1956).
21. W. M. Fairbank and G. K. Klauminzer, *Phys. Rev. B* **7,** 500 (1973).
22. C. M. Mc Donagh and B. Henderson, *J. Phys. C* **18,** 6419 (1985).
23. M. V. Johnston and J. C. Wright, *Anal. Chem.* **54,** 2503 (1982).
24. L. C. Porter and J. C. Wright, *J. Chem. Phys.* **77,** 2322 (1982).
25. D. S. Moore and J. C. Wright, *J. Chem. Phys.* **74,** 1626 (1981).
26. R. J. Hamers, J. R. Wietfeldt, and J. C. Wright, *J. Chem. Phys.* **77,** 683 (1982).
27. J. R. Wietfeldt and J. C. Wright, *J. Chem. Phys.* **83,** 4210 (1985).
28. J. R. Wietfeldt and J. C. Wright, *J. Chem. Phys.* **86,** 400 (1987).
29. S. I. Mho and J. C. Wright, *J. Chem. Phys.* **79,** 3962 (1983).
30. F. J. Weesner and J. C. Wright, *Phys. Rev. B* **33,** 1372 (1986).
31. J. C. Wright, *Cryst. Lattice Defects Amorphous Mater.* **12,** 505 (1985), and references therein.